Thymosin β_4 Binds Actin in an Extended Conformation and Contacts both the Barbed and Pointed Ends[†]

Daniel Safer,*[,‡] Tobin R. Sosnick,[§,||] and Marshall Elzinga[⊥]

Department of Cell and Developmental Biology, University of Pennsylvania, Philadelphia, Pennsylvania 19104-6058, Department of Biochemistry and Biophysics, Johnson Research Foundation, University of Pennsylvania, Philadelphia, Pennsylvania 19104-6059, and Department of Pharmacology, Institute for Basic Research, Staten Island, New York 10314-6399

Received January 27, 1997; Revised Manuscript Received March 14, 1997[⊗]

ABSTRACT: The β-thymosins are a family of highly polar peptides which serve *in vivo* to maintain a reservoir of unpolymerized actin monomers. *In vitro*, β-thymosins form 1:1 complexes with actin monomers and inhibit both polymerization and exchange of the bound nucleotide. Circular dichroism data indicate that free thymosin β_4 is predominantly unstructured, containing at most six residues of α-helix, and that up to six additional residues may adopt an α-helical conformation upon binding actin. NMR data indicate that many parts of thymosin β_4 are not in tight contact with actin. Contacts between specific residues in actin and thymosin β_4 were identified by zero-length cross-linking followed by isolation and sequencing of cross-linked peptides. After carbodiimide-mediated cross-linking, Lys-3 of thymosin β_4 was cross-linked to Glu-167 of actin, and Lys-18 of thymosin β_4 was cross-linked to one of the the N-terminal acidic residues of actin (Asp-1− Glu-4); the cross-linked actin residues lie within subdomains 3 and 1, respectively. These two contacts flank the α-helical region of thymosin β_4 and place it on the barbed end; thymosin β_4 can thus block actin polymerization sterically. After transglutaminase-mediated cross-linking, Lys-38 of thymosin β_4 was cross-linked to Gln-41 of actin, placing the C-terminal region of thymosin β_4 in contact with subdomain 2 on the pointed end; thymosin β_4 may sterically block actin polymerization at the pointed end as well as the barbed end of the monomer. The distance between the pointed-end and barbed-end contacts requires that the C-terminal half of thymosin β_4 be in a predominantly extended conformation.

Thymosin β_4 was first shown to be an actin-sequestering protein in human blood platelets, where it serves to maintain a pool of ∼280 μM unpolymerized actin monomers (*1*−*3*). Subsequently all other known β-thymosins from both vertebrate and invertebrate sources have been shown to bind actin monomers (*4*−*9*). Many other proteins have been described which form complexes with actin monomers, and the structures of three such complexes have been determined crystallographically: actin−DNase I[1] (*10*), actin−gelsolin segment 1 (*11*), and actin−profilin (*12, 13*). In each of these complexes, the actin-binding protein binds to a surface involved in intermonomer contacts in the actin filament, thus sterically inhibiting polymerization. The structure of another monomer-binding protein, destrin (also called actin depolymerizing factor), has recently been solved by NMR (*14*), showing that destrin is very similar in fold to gelsolin segment 1; a model was proposed for the actin−destrin complex, by positioning destrin on actin analogously with gelsolin segment 1.

In addition to modulating actin polymerization, actin monomer-binding proteins also influence the rate of exchange of the bound adenine nucleotide. DNase I (*15, 16*), gelsolin (*17, 18*), destrin (*19, 20*), and thymosin β_4 (*21*) inhibit nucleotide exchange, while profilin promotes exchange (*22*).

The present study was intended to determine whether thymosin β_4, like other monomer-binding proteins, inhibits actin polymerization by a steric mechanism, and to provide further information on the structural basis for the modulation of nucleotide exchange by monomer-binding proteins. In the absence of diffraction-quality crystals of the actin−Tβ_4 complex, our strategy was to identify residues involved in contacts between the two proteins, and then use the crystallographic structure of the actin monomer as a starting point for computational modeling of the complex. Since free thymosin β_4 is largely unstructured (*23*), it was first necessary to investigate its conformation when bound to actin. Preliminary results of this study were reported in abstract form (*24*).

[†] This research was supported by NIH Grant AR40840 and by a grant from the University of Pennsylvania Research Foundation to D.S. and V.T. Nachmias, and by grants from the New York State Office of Mental Retardation and Developmental Disabilities to M.E. T.R.S. was supported by NIH Grant GM31847 to S.W. Englander.

* To whom correspondence should be addressed. FAX: (215) 898-9871.

[‡] Department of Cell and Developmental Biology, University of Pennsylvania.

[§] Department of Biochemistry and Biophysics, University of Pennsylvania.

[||] Present address: Department of Biochemistry and Molecular Biology, University of Chicago, Chicago, IL 60637.

[⊥] Institute for Basic Research.

[⊗] Abstract published in *Advance ACS Abstracts,* May 1, 1997.

[1] Abbreviations: ADP, adenosine 5′-diphosphate; ATP, adenosine 5′-triphosphate; ATPγS, adenosine 5′-*O*-(3-thiotriphosphate); CD, circular dichroism; DNase I, deoxyribonuclease I; DTT, dithiothreitol; ESI, electrospray ionization; MALDI-TOF, matrix-assisted laser desorption ionization-time of flight; MS, mass spectroscopy; NMR, nuclear magnetic resonance; PAGE, polyacryamide gel electrophoresis; SDS, sodium dodecyl sulfate; Tβ_4, thymosin β_4; TFA, trifluoroacetic acid; Tris, tris(hydroxymethyl)aminomethane.

S0006-2960(97)00185-2 CCC: $14.00

EXPERIMENTAL PROCEDURES

Proteins. G-Actin was prepared from an acetone powder of rabbit skeletal muscle, following standard procedures (*25*). The concentration of actin was calculated using $E_{290} = 24.9$ mM^{-1} cm^{-1} (*3*). An affinity-purified polyclonal IgG against thymosin β_4 (*26*) was the generous gift of Vivianne T. Nachmias and Rajasree Golla.

Thymosin β_4 was prepared from bovine spleen as follows: in a typical preparation, 500 g of cryo-ground bovine spleen (PelFreez) was divided into 6 batches and added as a frozen powder to 5 volumes of 0.4 M perchloric acid at 4 °C, and then homogenized for 1 min using a Tekmar homogenizer at maximum speed. After removal of particulate material by centrifugation (25000*g* for 15 min), the extract was neutralized with cold 5 M KOH, and the potassium perchlorate precipitate was removed by centrifugation. The supernatant was adjusted to pH 2 by addition of 2 mL of TFA/L, filtered (0.45 μm), and loaded onto a column (2.5 × 20 cm) of Poros R2, 50 μm, (PerSeptive BioSystems), preequilibrated with 0.1% TFA. The column was flushed with 1 bed volume of 0.1% TFA, and then eluted with a 500 × 500 mL gradient from 0.1% TFA to 75% aqueous methanol. Loading and elution were performed at flow rates up to 600 mL/h. Fractions containing thymosin β_4 were identified by reverse-phase HPLC; for rapid screening, a 4.6 × 30 mm C18 column gave adequate resolution (A = 0.1% TFA, B = 0.08% TFA in CH_3CN, resolving gradient from 10 to 40% B in 3 min at 2 mL/min). Thymosin β_4 eluted from the Poros column just after the middle of the gradient, and did not correspond to a distinct peak in the UV trace at 230 or 280 nm. The fractions were pooled, concentrated by rotary evaporation, and mixed with 0.5 volume of 50 mM ammonium acetate, and the pH was adjusted to ~8 with dilute NH_4OH. The material was then loaded onto a 2.5 × 20 cm column of Dowex MP-1, 200−400 mesh, equilibrated with 50 mM ammonium acetate; after being flushed with 50 mM ammonium acetate, the column was eluted with a gradient of 300 × 300 mL, 50 mM ammonium acetate−0.2 M ammonium acetate + 0.2 M acetic acid. Two major peptide peaks (monitored at 220 or 230 nm) eluted in the gradient; the later one contained thymosin β_4, while the earlier peak, based on its actin-binding activity, contained one or more minor β-thymosins, possibly thymosin β_9 and/or thymosin β_9^{Met}. Final purification was performed by reverse-phase HPLC, using a Vydac 218TP510 column. At high concentrations, thymosin β_4 elutes from reverse-phase columns as a broad, irregular boundary, even though subsequent analytical runs show it to be homogeneous throughout. This "nonideal" behavior was minimized by using solvent A = 50 mM ammonium acetate, pH 6.5, B = CH_3CN, with the resolving gradient fron 12 to 20% B in 64 min at 2 mL/min; under these conditions, up to 40 mg could be loaded per run with good resolution. The pooled fractions were dialyzed against distilled water and lyophilized. The concentration of thymosin β_4 was measured by the bicinchonic acid procedure (*27, 2*).

Spectroscopy. Circular dichroism spectra were recorded using an Aviv 62DS spectrometer in a 2 mm path length cell at 5 °C. Data were recorded every 1 nm at 1 nm resolution. Samples contained 0 or 4 μM actin and 0, 3.8, or 7.6 μM thymosin β_4, in 2 mM potassium phosphate, 0.1 mM ATP, 0.1 mM $CaCl_2$, and 0.2 mM NaN_3, pH 7.4.

Proton NMR spectra were recorded on a Bruker AMX 500 MHz spectrometer in 5 mm tubes at 12 °C. A total of 256 transients of 4048 complex data points covering a spectral width of 9091 Hz were recorded. Water signal suppression was obtained using a WATERGATE pulsed gradient sequence (*28*). Spectra are reported with chemical shift in ppm from 3-(trimethylsilyl)propionate-d_6. Data were processed on a Silicon Graphics Indigo^2 running the Felix 2.30 software package. A 1 Hz line broadening was applied before Fourier transformation. After data processing, the residual water peak was eliminated by multiplying each spectrum by a buffer value of zero between 4.6 and 5.4 ppm and by a buffer value of 1 below 4.6 and above 5.4 ppm. Samples contained 0 or 160 μM actin and 0, 140, or 300 μM thymosin β_4, in 2 mM potassium phosphate, 0.1 mM ATP, 0.1 mM $CaCl_2$, and 0.2 mM NaN_3, pH 7.0.

Cross-Linking of Thymosin β_4 to Actin and Isolation of the Cross-Linked Complex. For carbodiimide-mediated cross-linking, a solution containing 50 μM G-actin and 50 μM thymosin β_4 in a depolymerizing buffer (3 mM triethanolamine hydrochloride, 0.2 mM ATP, 0.2 mM $CaCl_2$, and 0.2 mM NaN_3, pH 7.0) was brought to room temperature, and 1-ethyl-3-[3-(dimethylamino)propyl]carbodiimide and *N*-hydroxysuccinimide were added to give final concentrations of 0.5 mM. After stirring for 1 h at room temperature, the reaction was quenched by addition of Tris-HCl, pH 8.8, to a concentration of 15 mM. The reaction was then made 50 mM in KCl and 20 mM in $MgCl_2$ and stirred for 1 h at room temperature, causing most of the remaining non-cross-linked actin to polymerize. After centrifugation for 1 h at 200000*g*, the supernatant was diluted with an equal volume of the depolymerizing buffer and loaded onto a column of DEAE-cellulose (0.5−1 mL bed volume per milligram of protein in the cross-linking reaction) preequilibrated with 30 mM KCl, 10 mM imidazole hydrochloride, 0.2 mM ATP, 1 mM NaN_3, and 1 mM DTT, pH 7.0. After flushing briefly, the column was eluted with a gradient from 30 to 500 mM KCl in 10 mM imidazole hydrochloride, 0.2 mM ATP, 1 mM NaN_3, and 1 mM DTT, pH 7.0, in 5−6 column volumes; the eluate was collected in 60−80 fractions. Protein-containing fractions were identified by their A_{290} and were analyzed by SDS−PAGE. The procedure gave virtually complete separation of cross-linked actin−Tβ_4 from free thymosin β_4, and some additional separation of the cross-linked complex from the remaining free actin.

For transglutaminase-catalyzed cross-linking, guinea pig liver transglutaminase (Sigma) was added to a solution containing 50 μM G-actin and 50 μM thymosin β_4 in 10 mM Tris-HCl, 1 mM $CaCl_2$, 5 mM DTT, 0.5 mM ATP, and 0.2 mM NaN_3, pH 8.0, at a ratio of 5−10 mg of actin per unit of transglutaminase (*29*). Cross-linking was allowed to proceed overnight at 4 °C, and the cross-linked product was isolated by the same procedure used for carbodiimide-mediated cross-linking.

Cleavage of the Cross-Linked Complex and Isolation of Cross-Linked Peptides. Fractions containing at least 50% cross-linked material were pooled and S-carboxamidomethylated by addition of 15 mM Tris-HCl, pH 8.8, 20 mM iodoacetamide (10-fold excess over total thiol), and 8 M urea. After incubating for 60−90 min at room temperature in the dark, the material was dialyzed against ~50 volumes of 30 mM Na_2HPO_4, 10 mM NaH_2PO_4. To restrict subsequent tryptic digestion to arginine residues, lysine residues were blocked with citraconic anhydride (*30*); the material was then

dialyzed exhaustively against 0.5% NH_4HCO_3, 0.1% isobutyl alcohol, and digested with trypsin (TPCK-treated, Sigma or Worthington, ~5% by weight) for 16−22 h at 32−37 °C. To prevent cleavage at lysine residues after deblocking, digestion was terminated by incubating the digest for 1 h with a 5−10-fold excess of soybean trypsin inhibitor immobilized on agarose (Sigma). The digest was then filtered, lyophilized, redissolved in 1−2 mL, and fractionated by gel filtration on a 1.6 × 67 cm column of Superdex 75 prep grade (Pharmacia) in 0.2 M triethylammonium bicarbonate, pH 8.5, 0.1% isobutyl alcohol, at a flow rate of 40 mL/h; 2 mL fractions were collected. Peptide-containing fractions were identified by A_{230}, and formic acid was added to a final concentration of 2% in order to deblock lysine residues. After overnight incubation at room temperature, aliquots were evaporated to dryness, redissolved in 0.1 M potassium phosphate, pH 7.4, and spotted onto a covalent blotting membrane (Gelman Ultrabind US450 or Millipore Immobilon AV). Fractions containing cross-linked peptides were then identified by probing the membrane with an affinity-purified polyclonal antibody against thymosin β_4 followed by horseradish peroxidase-labeled secondary antibody (*26*), and were further fractionated by reverse-phase HPLC using an Isco chromatograph and a C18 column (Vydac 218TP54). Separations were performed both at pH 2 (A = 0.1% TFA, B = 0.08% TFA in CH_3CN) and at pH 6 (A = 13 mM ammonium acetate, pH 6; B = 10 mM ammonium acetate in 60% CH_3CN) at 1 mL/min, with gradient conditions as noted in the figure legends.

Further cleavage of cross-linked peptides was performed using the following proteases and conditions: chymotrypsin (Worthington), 5−10% w/w, at 32−37 °C for 16−22 h in 0.2 M NH_4HCO_3, 0.1% isobutyl alcohol; lysyl endopeptidase (Wako), at a molar ratio of 1:100, at 33 °C for 16 h, in 50 mM Tris-HCl, pH 9.0; *S. aureus* protease V8 (Sigma), 10% w/w, at 32−37 °C for 16−22 h in 50 mM sodium phosphate, pH 7.8; protease AspN (Sigma), 10% w/w, at 37° for 20 h in 50 mM sodium phosphate, pH 7.8.

Characterization of Peptides. Peptides of interest were initially characterized by mass spectroscopy at the Protein Chemistry Facility of the Department of Pathology and Laboratory Medicine, University of Pennsylvania, using the MALDI-TOF method. Additional mass spectroscopy was performed, where noted, by the electrospray ionization method. Some peptides were further characterized by amino acid analysis at the Protein Microchemistry Core Facility of the Wistar Institute. N-Terminal sequencing was performed using ABI sequencers at the Institute for Basic Research and at the Wistar and the University of Pennsylvania protein chemistry facilities. The isodipeptide γGlu-ϵLys (Sigma) was used as a standard on the sequencer for the isodipeptide released by N-terminal sequencing of cross-linked peptides.

Molecular Modeling. Molecular modeling was performed at the University of Pennsylvania Cancer Center Computer Facility using Insight*II* on a Silicon Graphics Indigo workstation. Actin coordinates were taken from the Brookhaven Protein Data Base file 1ATNA.

RESULTS

Spectroscopic Studies of Free and Actin-Bound Thymosin β_4. The far-UV circular dichroism spectra of free and actin-bound thymosin β_4 are shown in Figure 1. This region of the spectrum is sensitive to the time-averaged secondary structure of the polypeptide chain. The spectrum of free thymosin β_4 is dominated by the deep trough at 200 nm, indicating that thymosin β_4 is predominantly in a random coil conformation (*31*). The nonzero value at 222 nm indicates that part of the structure may not be an ideal random coil; the observed value of θ_{222} could correspond to as much as 15% α-helix, or 6 out of 43 residues [100% helix = 32 000 deg $dmol^{-1}$ cm^{-2} (*31*)]. The current spectra are similar to those of Czisch et al. (*23*).

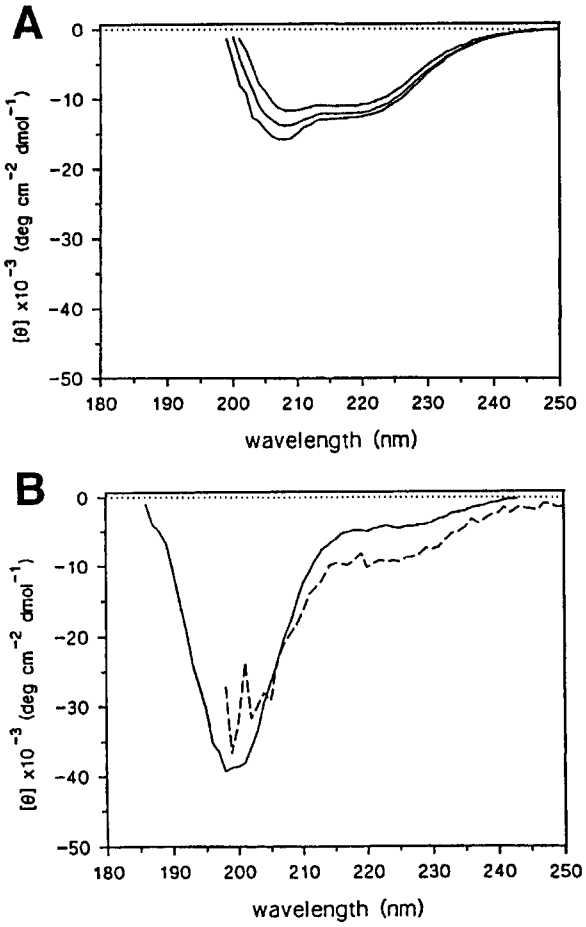

FIGURE 1: Circular dichroism spectra of free and actin-bound thymosin β_4. (A) CD spectra of 4 μM G-actin (upper curve), 4 μM G-actin plus 3.8 μM thymosin β_4 (middle curve), and 4 μM G-actin plus 7.6 μM thymosin β_4 (lower curve). (B) CD spectra of 3.8 μM thymosin β_4 alone (solid line) and in the presence of 4 μM actin (dashed line). The CD spectrum of thymosin β_4 in the presence of actin was calculated by subtracting the spectrum of actin alone (Figure 1A, upper curve) from the spectrum of actin plus thymosin β_4 (Figure 1A, middle curve).

The CD spectrum of thymosin β_4 was also measured in the presence of equimolar actin (Figure 1). The spectrum of bound thymosin β_4 alone was obtained by subtracting the actin signal measured under identical conditions from the spectrum of the complex. Again, the thymosin β_4 spectrum indicated a predominantly random coil structure, but the increased depth (roughly doubled) of the trough at 222 nm indicated the formation of some additional ordered structure upon binding actin. The change in ellipticity at 222 nm could be accounted for by six additional residues of α-helix, though the CD signal can also have contributions from β-sheet and other structures (*32*). If the value of θ_{222} for actin-bound thymosin β_4 resulted entirely from α-helix, a maximum of 12 residues would be α-helical.

As a control for this sensitive difference measurement, a second molar aliquot of thymosin β_4 was added to the

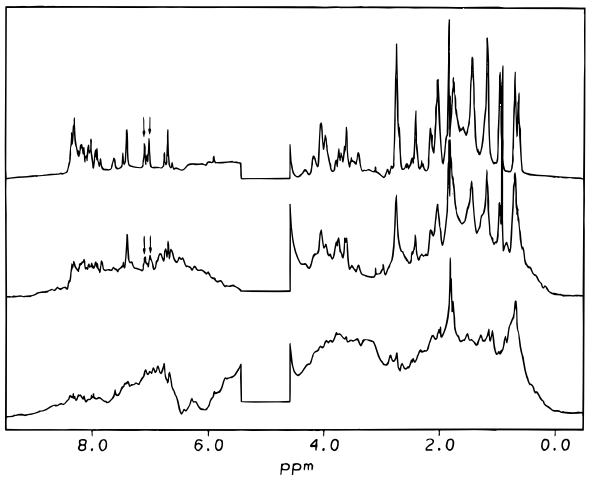

FIGURE 2: ^{1}H-NMR spectra of actin and thymosin β_4. Upper curve, 140 μM thymosin β_4; middle curve, 140 μM thymosin β_4 plus 160 μM actin; lower curve, 160 μM actin. The arrows indicate the phenylalanine resonances. Resonances between 0 and 5 ppm are derived from side chain aliphatic protons.

equimolar mixture. As anticipated from the 1:1 binding stoichiometry, the increment in θ_{222} from the second mole equivalent of thymosin β_4 was about half that of the first mole equivalent, and equal to θ_{222} for the same concentration of free thymosin β_4; i.e., the excess thymosin β_4 did not become more ordered.

One-dimensional ^{1}H NMR spectra of free thymosin β_4 showed narrow line widths and low dispersion (Figure 2, upper curve), and are consistent with a predominantly random coil structure which is highly mobile on the NMR time scale (*33*). The spectrum of actin alone (Figure 2, lower curve) is typical of any large protein, and consistent with earlier published spectra (*34*, *35*), showing very few sharp resonances due to the slow molecular tumbling rate. The spectrum of thymosin β_4 bound to actin, after subtraction of the actin signal (Figure 2, middle curve), is very similar to the spectrum of free thymosin β_4 (Figure 2, upper curve). If thymosin β_4 were largely immobilized when bound to actin, its spectrum in the bound state would resemble the actin spectrum, with most peaks strongly broadened or unresolvable. Instead, most thymosin β_4 resonances are still resolvable, though broader, and only a few resonances in the spectrum of actin-bound thymosin β_4 show clear changes in shift, indicating changes in the local environment of the corresponding protons. Broadening is particularly evident for the phenylalanine resonances at 7.3 ppm. Overall, the minimal change in chemical shift for most resonances indicates that most of the observable protons undergo little change in local environment when thymosin β_4 binds actin, while their effective tumbling rate, judged from the moderate increase in resonance line widths, is intermediate between those of free thymosin β_4 and actin.

Two-dimensional NMR studies have shown that free thymosin β_4 does not have a unique conformation in aqueous solution; while residues 5−16 tend to adopt an α-helical structure, the rest of the molecule (residues 1−4 and 17−43) is predominantly unstructured (*23*). The CD data presented above indicate the formation of additional ordered structure when thymosin β_4 binds actin, while the NMR data indicate that at least some of this change in structure occurs in thymosin β_4 rather than in actin. Overall, the published spectroscopic results and those presented above suggest that in the actin−Tβ_4 complex, up to 12 residues of thymosin β_4, possibly residues 5−16, are in an α-helical conformation, while the rest of the peptide is predominantly in a random coil conformation. The high mobility of thymosin β_4 when bound to actin, and the relatively small change in local environment for most of the observable protons, suggests that, on average, the side chains of thymosin β_4 are not tightly packed on actin.

Identification of Interresidue Contacts by Cross-Linking. Strategy. "Zero-length" cross-linking was used to create isopeptide linkages between side chains on actin and thymosin β_4. This approach is based on the premise that certain noncovalent interactions between acidic and basic residues in the native structure can be converted to covalent bonds by cross-linking. The overall scheme for cross-linking, cleavage, and isolation of cross-linked peptides is shown in Figure 3. To facilitate isolation of cross-linked peptides, the cross-linked complex was digested with trypsin after reversibly blocking lysine residues; under these conditions, actin was cleaved at arginine residues, while thymosin β_4, which lacks arginine, was uncleaved. After the initial chromatographic step and deblocking of lysine residues, fractions containing cross-linked peptides were identified by their reactivity with an antibody to thymosin β_4. Individual peptides were then isolated by reverse-phase HPLC. Presumptive cross-linked peptides were initially characterized by mass spectroscopy, followed by sequencing and/or amino acid analysis; cross-linked residues were identified unambiguously after further cleavage of the cross-linked peptides and characterization of the cleavage products.

As shown schematically in Figure 3A, the major cross-linked product following carbodiimide-mediated cross-linking and cleavage at arginine residues consisted of thymosin β_4 plus actin residues 1−28; after further cleavage with chymotrypsin and lysyl endopeptidase and characterization of the products, Lys-18 of thymosin β_4 was shown to be cross-linked to one of the four acidic residues at the actin N-terminus. The minor product from carbodiimide-mediated cross-linking and initial cleavage is shown in Figure 3B; the cross-linked fragment contained thymosin β_4 plus actin residues 148−173. After further cleavage with proteases V8 and AspN and characterization of the fragments, Lys-3 of thymosin β_4 was shown to be cross-linked to actin Glu-167. The product of transglutaminase-mediated cross-linking is shown in Figure 3C; the initial cleavage product consisted of actin residues 40−62 plus thymosin β_4. After further cleavage with lysyl endopeptidase and N-terminal sequencing, actin Gln-41 was found to be cross-linked to Lys-38 of thymosin β_4. Details of these procedures are given below and in Figures 4 and 5.

Isolation and Characterization of Cross-Linked Peptides. Carbodiimide-mediated cross-linking generates isopeptide linkages between the side chains of lysine and glutamate or aspartate residues. The scheme for isolation of carbodiimide-cross-linked peptides is shown in Figure 4A. This procedure was carried out several times with minor variations, and the same major cross-linked products (based on retention time and mass) were isolated in each of several experiments. Representative chromatograms are taken from several preparations.

Under the conditions described, about 20−30% of the protein in the reaction became cross-linked. Higher yields of cross-linked product could be obtained by increasing the concentration of cross-linking reagents or the duration of the reaction, but this resulted in a large fraction of high molecular

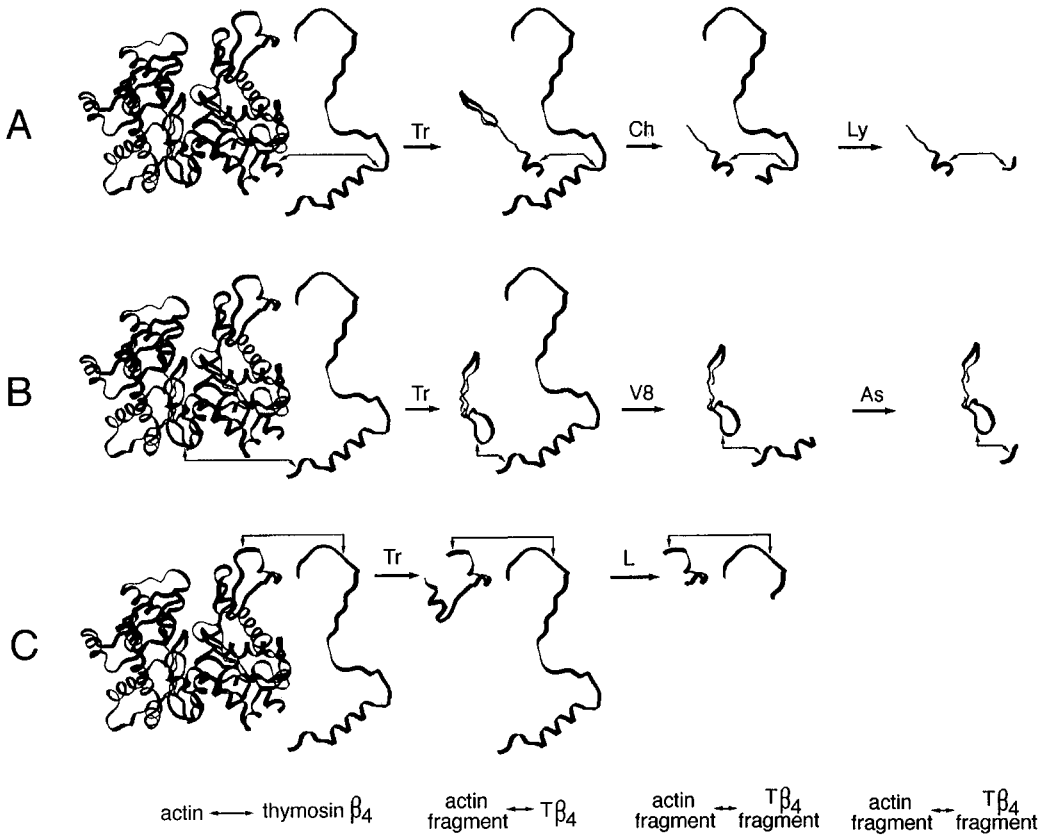

FIGURE 3: Overall scheme for zero-length cross-linking and the isolation of cross-linked peptides. Proteases are indicated as Tr (trypsin), Ch (chymotrypsin), Ly (lysyl endopeptidase), V8, and As (AspN). Double-headed arrows indicate cross-links. (A) The major site of carbodiimide-mediated cross-linking was between Lys-18 of thymosin β_4 and one of the four acidic residues at the actin N-terminus. Tryptic cleavage (after reversible blocking of lysine side chains by citraconylation) released the cross-linked peptide consisting of thymosin β_4 plus actin residues 1−28. Further cleavage with chymotrypsin produced two cross-linked peptides, both containing actin residues 1−8; one contained Tβ_4 residues 13−43, and was used for sequence analysis, identifying Lys-18 as the cross-linked residue on Tβ_4. The second (not shown in this figure) contained actin residues 1−8 plus Tβ_4 residues 18−43, and was redigested with lysyl endopeptidase to yield the cross-linked fragment consisting of actin residues 1−8 plus Tβ_4 residues 18 and 19. (B) The minor site of carbodiimide-mediated cross-linking was between actin Glu-167 and Tβ_4 Lys-3. Citraconylation and tryptic cleavage released a mixture of cross-linked products consisting of thymosin β_4 plus an actin peptide beginning at Thr-148 and ending at Tyr-169, His-173, or Arg-177. The peptide containing actin residues 148−173 was redigested with protease V8, yielding the cross-linked fragment consisting of actin residues 155−173 plus Tβ_4 residues 1−8. N-Terminal sequencing showed that the cross-linked residue on actin was Glu-167. Further cleavage with protease AspN yielded the cross-linked fragment consisting of actin residues 155−173 plus Tβ_4 residues 1−4, identifying Lys-3 as the cross-linked residue on thymosin β_4. (C) The site of transglutaminase-mediated cross-linking was between actin Gln-41 and Tβ_4 Lys-38. Citraconylation and tryptic cleavage released the cross-linked peptide consisting of actin residues 40−62 plus thymosin β_4. Further cleavage with lysyl endopeptidase yielded the cross-linked fragment consisting of actin residues 40−50 plus Tβ_4 residues 32−43. N-Terminal sequencing identified both of the cross-linked residues.

weight, heterogeneous products after tryptic digestion, which reduced the subsequent recovery of sequenceable cross-linked peptides (data not shown). By limiting the extent of cross-linking and removing most of the non-cross-linked protein by polymerization and ion-exchange chromatography, it was possible to obtain preparations which were >50% cross-linked, from which products with single cross-links could be recovered in good yield.

Sites of Carbodiimide-Mediated Cross-Linking. Following arginine-specific digestion and gel filtration, nearly all the immunoreactive material eluted in a single peak well behind the void volume and well-resolved from the bulk of the digest (Figure 4B). When this material was fractionated by reverse-phase HPLC (Figure 4C,D,E), most of it consisted of a set of partially-resolved components ranging in mass from 7850 to about 8000 Da. Comparison with the masses predicted for actin peptides cross-linked to thymosin β_4 showed that the closest match was to actin residues 1−28 plus thymosin β_4: the predicted mass, 7868 Da, was an exact match (within experimental error) for the observed mass of 7870 Da for one of the major components of this set. Since the N-termini of both actin and thymosin β_4 are blocked, this component was not sequenced directly. Chymotryptic cleavage of this set of cross-linked peptides yielded two major products (Figure 4F): a fragment which exactly matched, in mass and retention time, the N-terminal chymotryptic fragment (residues 1−12) of unmodified thymosin β_4; and a pair of fragments about 3867 and 4457 Da. The 3867 Da fragment approximately matched the mass predicted for a cross-linked peptide consisting of actin residues 1−8 plus thymosin β_4 residues 18−43, while the 4457 Da fragment approximately matched the mass predicted for actin residues 1−8 plus thymosin β_4 residues 13−43. The relative proportions of the 3867 and 4457 Da fragments varied in different digests. Amino acid analysis of both the 3867 Da and the 4457 Da fragments matched the predicted compositions (Table 1). Ten cycles of N-terminal sequencing of the 4457 Da fragment gave the sequence of thymosin β_4 beginning at residue 13; Lys-18 was absent, while Lys-14, Lys-16, and Lys-19 were detected in good yield (Table 2A). The failure to detect Lys-18 of thymosin β_4 indicated that this residue was modified and therefore the presumptive site of cross-linking. The corresponding cross-linked residue in the actin sequence could be Asp-1, Glu-2, Asp-3, or Glu-4; these possibilities

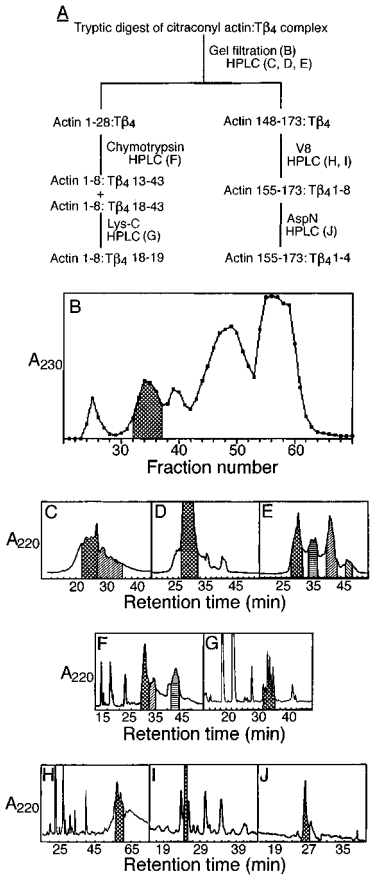

FIGURE 4: Isolation of carbodiimide-cross-linked peptides. (A) Summary of the isolation scheme. (B) Fractionation of the tryptic digest by gel filtration on Superdex 75. Fractions 32−37 (cross-hatched) were found to contain cross-linked peptides by reactivity with the anti-Tβ_4 antibody. (C) Fractionation of the cross-linked material from Figure 4B by HPLC at pH 2; gradient from 21.7% B at 10 min to 33.3% B at 45 min. The shaded region contained the bulk of the cross-linked material and was used for further fractionation. (D) Refractionation of the cross-linked material from Figure 4C (cross-hatched region) by HPLC at pH 6; gradient from 25% B at 15 min to 50% B at 55 min. The resulting peak (crosshatched) contained the cross-linked peptide actin 1−28−Tβ_4. (E) Refractionation of the cross-linked material from Figure 4C (striped region) by HPLC at pH 6; gradient from 25% B at 15 min to 50% B at 55 min. The shaded peaks contained the following cross-linked peptides: actin 1−28:Tβ_4 (cross-hatched); actin 148−169:Tβ_4 (horizontal stripes); actin 148−173:Tβ_4 (right diagonal stripes); actin 148−177:Tβ_4 (left diagonal stripes). (F) The cross-linked material from Figure 4D was digested with chymotrypsin and fractionated by HPLC at pH 2; gradient from 12.3% B at 10 min to 27.3% B at 55 min. The shaded peaks contained: actin 1−8:Tβ_4 18−43 (cross-hatched); actin 1−8:Tβ_4 13−43 (diagonal stripes); and Tβ_4 1−12 (horizontal stripes). (G) The cross-hatched peak from Figure 4F was digested with lysyl endopeptidase and fractionated by HPLC at pH 2; gradient from 12% B at 10 min to 22% B at 50 min. The resulting set of peaks at 32−36 min (cross-hatched) contained actin 1−8:Tβ_4 18−19. (H) The peak from Figure 4E containing actin 148−173:Tβ_4 (right diagonal stripes) was digested with protease V8 and fractionated by HPLC at pH 2; gradient from 9.3% B at 15 min to 29.3% B at 75 min. The cross-hatched peak contained actin 155−173:Tβ_4 1−8. (I) The cross-linked material from Figure 4H was refractionated by HPLC at pH 6; gradient from 26.7% B at 15 min to 46.7% B at 45 min. An aliquot of the cross-hatched peak was sequenced. (J) A second aliquot of the cross-hatched peak from Figure 4I was digested with endoprotease AspN and fractionated by HPLC at pH 6; gradient from 26.7% B at 15 min to 43.3% B at 40 min. The cross-hatched peak contained actin 155−173:Tβ_4 1−4.

could not be distinguished by sequencing because the N-terminus of actin is blocked, and the peptide resisted further proteolysis.

In a subsequent experiment, the 3867 Da chymotryptic fragment, corresponding to actin residues 1−8 plus thymosin β_4 residues 18−43, was redigested with lysyl endopeptidase (Figure 4G). This yielded a major product consisting of four or more closely-spaced peaks, all of mass 1192 Da (determined by ESI-MS). The observed mass is in exact agreement with the calculated mass of actin residues 1−8 plus Tβ_4 Lys-18-Lys-19, confirming that the cross-link is to Lys-18 of thymosin β_4. The fact that this material chromatographed as more than one peak may indicate two or more alternative sites of cross-linking in the first four actin residues.

Two additional cross-linked peptides were isolated from the arginine-specific digest in each of three experiments, with observed masses of 7250 and 7671 Da (Figure 4E). Sequencing showed that the 7250 Da fragment contained actin residues 148−169 (data not shown), and its mass and amino acid composition confirmed that it consisted of this actin sequence plus thymosin β_4 (Table 1). The mass and amino acid composition of the 7671 Da peptide were consistent with thymosin β_4 plus actin residues 148−173, and this identification was confirmed by N-terminal sequencing after further cleavage with protease V8 (Table 2B, discussed below). It is not clear why tryptic cleavage occurred at these anomalous sites (Tyr-169 and His-173), but the same result was obtained in three different experiments with trypsin from two different sources. An additional peptide of mass 8143 Da, corresponding to the product expected for arginine-specific cleavage (thymosin β_4 plus actin residues 148−177), was isolated in much smaller quantities and was not characterized further.

The actin sequence 148−173 contains no lysine residues; thus, cross-linking must involve a lysine residue in thymosin β_4 and one of the three carboxylic residues in this actin sequence, Asp-154, Asp-157, or Glu-167. To identify the cross-linked residues, the 7671 Da cross-linked peptide was cleaved with V8 protease, yielding a major fragment of 2966 Da (Figure 4H,I). N-Terminal sequencing (15 cycles) showed that this fragment begins at actin residue 155; Asp-157 was detected in good yield, while Glu-167 was absent, indicating that Glu-167 is the cross-linked residue on actin (Table 2B). Since no thymosin β_4 sequence was observed due to the blocked N-terminus, the cross-linked residue on thymosin β_4 could not be identified directly. An aliquot of the 2966 Da fragment was then redigested with endoprotease AspN (Figure 4J) and characterized by mass spectroscopy and amino acid analysis (Table 1). Both the mass and the amino acid composition were in close agreement with the predicted values for actin residues 155−173 plus thymosin β_4 residues 1−4. This fragment of thymosin β_4 contains a single lysine residue at position 3, indicating that the cross-link is between actin Glu-167 and Tβ_4 Lys-3.

As noted above, the observed masses of the cross-linked products frequently showed discrepancies from the masses predicted from sequence analysis; the product corresponding to thymosin β_4 plus actin residues 1−28, obtained after cleavage at arginine residues, was particularly heterogeneous in this regard. However, the cross-linked fragments produced after further digestion of this set of fragments, using chymotrypsin followed by lysyl endopeptidase, showed less heterogeneity and less deviation from predicted mass than the initial set of cross-linked peptides obtained from arginine-specific digestion. This result suggests that the observed heterogeneity probably resulted from side reactions during

Table 1: Mass and Amino Acid Composition of Carbodiimide-Cross-Linked Peptides[a]

	peptide							
	actin 1−8:Tβ_4 13−43		actin 1−8:Tβ_4 18−43		actin 148−169:Tβ_4 1−43		actin 155−173:Tβ_4 1−4	
residue	calcd	obsd	calcd	obsd	calcd	obsd	calcd	obsd
Asp, Asn	4	3.87	3	3.11	7	7.07	3	2.85
Glu, Gln	11	10.61	11	10.46	12	11.83	1	1.35
CMCys	0	0.51	0	0.48	0	0.51	0	0.00
Ser	3	3.04	2	1.82	5	4.93	2	1.99
Gly	1	1.32	1	1.11	5	5.21	3	2.93
His	0	0.00	0	0.00	1	0.93	2	1.66
Arg	0	0.00	0	0.00	0	0.00	0	0.14
Thr	5	4.71	5	3.82	6	4.92	1	1.33
Ala	2	2.27	2	*2.00*	2	2.06	1	1.12
Pro	2	2.25	2	2.00	4	3.89	3	2.51
Tyr	0	0.04	0	0.02	2	1.82	2	1.53
Val	0	0.08	0	0.02	3	2.60	2	1.75
Met	0	0.28	0	0.07	1	1.35	0	0.00
Ile	1	1.14	1	0.92	4	3.18	1	0.83
Leu	3	*3.00*	2	2.05	3	*3.00*	1	*1.00*
Phe	0	0.22	0	0.07	1	1.01	0	0.12
Lys	7	7.03	5	4.89	9	7.57	1	0.98
total	39	40.37	34	33	65	61.88	23	22.09
mass	4430	4457	3858	3867	7253	7262	2496	2503

[a] In each amino acid analysis, the experimental data were normalized against the value shown in italics.

Table 2: Sequence Data for Carbodiimide-Cross-Linked Peptides

(A) Data for the 4457 Da Cross-Linked Peptide

Tβ_4 sequence 13−22	sequencer cycle	observed sequence[a] A	(pmol)	B	(pmol)
Asp	1	Asp	(29.4)	Gly	(3.2)
Lys	2	Lys	(22.6)	Asp	(2.4)
Ser	3	Ser	(3.3)	Lys	(2.0)
Lys	4	Lys	(10.7)	Glu	(3.1)
Leu	5	Leu	(19.9)	Lys	(1.6)
Lys	6			Gln	(1.8)
Lys	7	Lys	(7.8)	Glu	(2.8)
Thr	8	Thr	(4.3)	Lys	(2.5)
Glu	9	Glu	(16.6)	Gln	(1.8)
Thr	10	Thr	(3.4)	Glu	(3.5)

(B) Data for the 2966 Da Cross-Linked Peptide

actin sequence 155−169	sequencer cycle	observed sequence A	(pmol)	B	(pmol)
Ser	1	Ser	(38.0)	Asp	(32.6)
Gly	2	Gly	(58.3)		
Asp	3	Asp	(29.9)	Gly	(13.4)
Gly	4	Gly	(47.9)	Asp	(20.3)
Val	5	Val	(54.9)	Gly	(17.2)
Thr	6	Thr	(28.3)	Val	(21.1)
His	7	His	(35.0)	Asp	(14.6)
Asn	8	Asn	(36.4)	His	(19.3)
Val	9	Val	(34.8)	Asn	(16.3)
Pro	10	Pro	(24.2)	Val	(20.1)
Ile	11	Ile	(20.8)	Pro	(16.7)
Tyr	12	Tyr	(22.2)	Phe	(21.8)
Glu	13			Tyr	(15.0)
Gly	14	Gly	(11.6)	Tyr	(9.9)
Tyr	15	Tyr	(12.7)	Gly	(10.2)

[a] Column A reports the major residue released at each cycle. Column B reports residues which are thought to result from incomplete release at previous cycles, or from contamination.

cross-linking, or from incomplete release of the citraconyl groups during deblocking (*30*), occurring at a number of side chains, and not from heterogeneity in the site or number of cross-links.

Site of Transglutaminase-Catalyzed Cross-Linking. Transglutaminase generates isopeptide linkages between the side chains of lysine and glutamine residues (*36*). The arginine-specific digest of the transglutaminase-cross-linked complex fractionated in much the same way as the carbodiimide-cross-linked material, but yielded a more homogeneous set of cross-linked peptides (Figure 5). The major product had a mass of 7460, in reasonable agreement with the predicted mass of 7453 for thymosin β_4 plus actin residues 40−62. N-Terminal sequencing showed the predicted actin sequence beginning at His-40, with Gln-41 absent (data not shown). To identify the cross-linked residues, the cross-linked peptide was redigested with lysyl endopeptidase. One major cross-linked fragment was isolated from the digest (Figure 5E). The observed mass of 2492 Da was in good agreement with the calculated mass (2502 Da) of actin residues 40−50 plus thymosin β_4 residues 32−43. N-Terminal sequencing gave two major residues at each cycle, as predicted for a cross-linked peptide with two free N-termini (Table 3). The first six cycles correspond to the expected sequences of actin beginning at His-40 plus thymosin β_4 beginning at Glu-32, with actin Gln-41 absent at cycle 2. At cycle 7, actin Gly-46 was released, along with the Glu-Lys isodipeptide. Glu rather than the expected Gln was released at cycle 8, probably as a result of deamidation by transglutaminase. The absence of actin Gln-41 at cycle 2 and the release of the isodipeptide rather than Tβ_4 Lys-38 at cycle 7 indicate that the transglutaminase-catalyzed cross-link is between actin Gln-41 and Tβ_4 Lys-38.

Additional evidence for the interaction of thymosin β_4 with this region on subdomain 2 of the actin monomer was provided by two lines of data. First, actin was fluorescently labeled at Gln-41 by transglutaminase-catalyzed incorporation of dansylcadaverine (*29*). Addition of equimolar thymosin β_4 to this labeled preparation resulted in quenching of the fluorescence at 520 nm by ~17%, indicating that thymosin β_4 changed the environment of the fluorophore. Second, several experiments have shown that DNase I inhibits the binding of thymosin β_4 to actin. Addition of equimolar DNase I to the actin−Tβ_4 complex results in the formation of the actin−DNase I complex plus free thymosin β_4, as demonstrated both by nondenaturing PAGE and by gel filtration (data not shown). Similarly, a study using equilibrium centrifugation found that the affinity of thymosin

Table 3: Sequence Data for the 2492 Da Transglutaminase-Cross-Linked Peptide

actin sequence 40−50	Tβ_4 sequence 32−43	sequencer cycle	observed sequence[a] A	(pmol)	B	(pmol)	C	(pmol)	D	(pmol)
His	Glu	1	His	(104)	Glu	(124)				
Gln	Thr	2			Thr	(65.5)	His	(29.3)	Glu	(27.1)
Gly	Ile	3	Gly	(78.1)	Ile	(112)	Thr	(16.9)	Glu	(9.0)
Val	Glu	4	Val	(106)	Glu	(60.8)	Ile	(50.8)	Gly	(24.8)
Met	Gln	5	Met	(77.7)	Glu	(65.9)	Val	(25.7)	His	(14.0)
Val	Glu	6	Val	(83.4)	Glu	(84.6)	Met	(22.9)	Gly	(7.5)
Gly	Lys	7	Gly	(46.2)	*E-K*	(20.6)	Glu	(57.6)	Val	(23.7)
Met	Gln	8	Met	(48.8)	Gln	(14.8)	Glu	(36.9)	*E-K*	(21.3)
Gly	Ala	9	Gly	(32.7)	Ala	(16.9)	Glu	(27.8)	Gln	(20.7)
Gln	Gly	10	Gln	(24.2)	Gly	(18.8)	Glu	(18.9)	Ala	(17.5)

[a] Columns A and B report the major residues released at each sequencer cycle. Columns C and D report residues which are thought to result from incomplete release at previous cycles, or from contamination. *E-K* indicates the cross-linked isodipeptide γGlu-ϵLys, which coeluted with Phe.

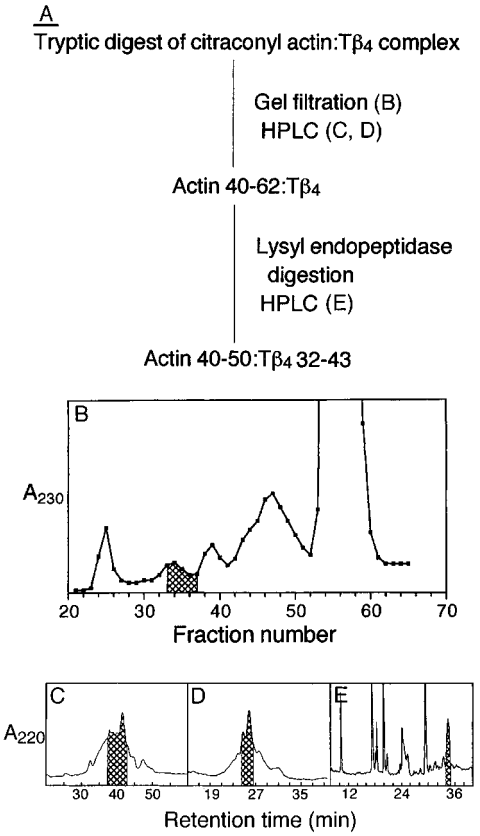

FIGURE 5: Isolation of the transglutaminase-cross-linked peptide. Fractions containing cross-linked material, as identified by immunoreactivity, are cross-hatched. (A) Summary of the isolation scheme. (B) Gel filtration of the tryptic digest on Superdex 75. (C) Fractionation of cross-linked material from Figure 5B by HPLC at pH 2; gradient from 19% B at 20 min to 29% B at 60 min. (D) Refractionation of the cross-linked material from Figure 5C by HPLC at pH 6; gradient from 25% B at 15 min to 37.5% B at 40 min. The cross-hatched peak contained the cross-linked peptide, actin 40−62:Tβ_4. (E) The cross-linked material from Figure 5D was digested with lysyl endopeptidase and fractionated by HPLC at pH 2; gradient from 7.5% B at 8 min to 23.5% B at 40 min. The cross-hatched peak contained the cross-linked peptide, actin 40−50:Tβ_4 32−43, and was sequenced.

β_4 for actin is reduced by about 2 orders of magnitude in the presence of equimolar DNase I (*8*). These results indicate that the binding site for thymosin β_4 on actin overlaps the binding site for DNase I.

A model for the actin−Tβ_4 complex which incorporates the available data is shown in Figure 6.

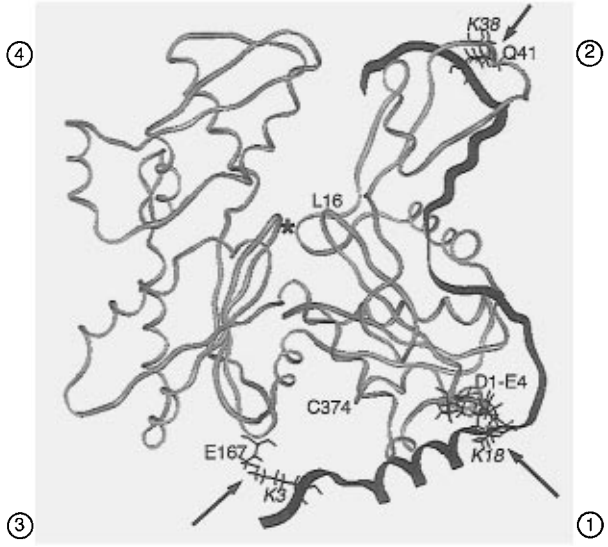

FIGURE 6: Preliminary model for the actin−Tβ_4 complex. The actin monomer is shown as a tube in the commonly-used orientation (Kabsch et al., 1990; McLaughlin et al., 1993), with the barbed end at the bottom. The subdomains are indicated by the circled numbers. Thymosin β_4 is shown as a solid black ribbon, with its N-terminus at the bottom of the figure. Thymosin β_4 residues 5−16 are shown in an α-helical conformation, based on spectroscopic data as discussed in the text. The remainder of the thymosin β_4 structure was fit manually to the actin monomer so as to allow contacts between side chains involved in cross-links, and to place the hydrophobic face of the α-helical segment in contact with the hydrophobic pocket on the barbed end of actin; the conformation of thymosin β_4 outside the α-helical region must be predominantly extended but is not known in detail. Side chains are shown only for residues involved in cross-links (arrows). Residues are identified by single-letter code and number; residues in thymosin β_4 are in italics. The asterisk indicates the position of the bound nucleotide.

DISCUSSION

Conformation of Thymosin β_4 Bound to Actin. The published NMR studies of thymosin β_4 have shown that, under physiological conditions, residues 5−16 tend to adopt an α-helical conformation, though this represents an average rather than a stable structure; the rest of the molecule remains unfolded, without a unique conformation (*23*). NMR spectra also indicate that a region near the C-terminus shows a slight tendency toward α-helical structure at low temperatures, but not at physiological temperatures, although CD spectra show no significant change in overall α-helix content with temperature (*23*). The CD spectra presented here indicate that the binding of thymosin β_4 to actin is accompanied by an increase in nonrandom structure, while the NMR data

indicate some changes in the conformation of thymosin β_4 upon binding. The most straightforward interpretation is that actin binding tends to stabilize the nonrandom structure in thymosin β_4, consistent with an increase of ~6 residues of α-helix; we cannot exclude the possibility that conformational changes occur in actin as well. The present data effectively rule out a predominantly α-helical structure, such as that induced by trifluoroethanol (*37*), for thymosin β_4 bound to actin. We cannot distinguish whether the additional structured residues in the actin-bound form are within residues 5−16 or in a different part of the sequence on the basis of spectroscopic data. However, a recent study (*38*) using designed sequence variants of thymosin β_4 showed that substitutions which stabilize the α-helix between residues 5 and 16 tend to favor actin binding, while substitutions that destabilize the helix inhibit binding; a synthetic peptide corresponding to thymosin β_4 residues 5−16 has also been shown to have a higher affinity for actin when in an α-helical conformation (*39*). These results suggest that the increased nonrandom structure observed in actin-bound thymosin β_4 probably corresponds to stabilization of the α-helical region in residues 5−16.

Contacts between Actin and Thymosin β_4 and Implications for Three-Dimensional Structure. We have found three sites of cross-linking between thymosin β_4 and actin: two on the barbed end of the actin monomer, Tβ_4 Lys-3 to actin Glu-167 and Tβ_4 Lys-18 to one of the first four residues at the actin N-terminus; and one on the pointed end of the monomer, Tβ_4 Lys-38 to actin Gln-41 (Figures 3 and 6). All of the lysine residues on Tβ_4 which are involved in cross-linking are conserved in all the known β-thymosins.

The 2 contacts identified on the barbed end of the actin monomer, Tβ_4 Lys-3 to actin Glu-167 and Tβ_4 Lys-18 to actin residues 1−4, are 25−30 Å apart (Figure 6); the 12 residue α-helical region of thymosin β_4 is between these 2 contacts and would have a length of ~18 Å. In order to span the distance between the points of cross-linking, the residues flanking the α-helical region would need to be in an extended conformation. The α-helical region has a hydrophobic face consisting of Met-6, Ile-9, and Phe-12, which is likely to be the face in contact with actin (*38*); the enhancement of actin's intrinsic tryptophan fluorescence induced by the binding of thymosin β_4 (*7*) suggests that part of this face contacts actin Trp-356. The N-terminal region of thymosin β_4 is thus situated to compete with other proteins that bind the barbed end of the monomer, as reported for profilin (*21*) and as we have observed for vitamin D-binding protein (Safer, unpublished results).

The C-terminal region of thymosin β_4 contacts actin on subdomain 2, with Tβ_4 Lys-38 adjacent to actin Gln-41. Independent evidence for the interaction of thymosin β_4 with this region on actin, which is within the binding site for DNase I (*10*), is provided by the observation that DNase I inhibits the binding of thymosin β_4 to actin. In addition, thymosin β_4 quenches the fluorescence of a dansyl probe bound to Gln-41; the fluorescence of the dansyl probe at Gln-41 is similarly altered by the binding of other proteins in its vicinity, by actin polymerization (*29*), by binding of DNase I (*40*), or by binding an anti-dansyl antibody (*41*), though in all these cases the fluorescence is enhanced by binding.

Both the cross-linking and the spectroscopic data were obtained using actin in the Ca^{2+} form. Recent studies of actin structure have shown that the substitution of Ca^{2+} for Mg^{2+}specifically influences the environment of fluorophores bound to Gln-41 (*40, 54*), suggesting that the interaction between thymosin β_4 and actin on subdomain 2 might be affected by the divalent cation bound to actin. However, the fact that the actin sequestering activity of thymosin β_4 is Ca^{2+}-insensitive (*3*) suggests that the substitution of Ca^{2+} for Mg^{2+} should not have a major effect on the structure of the complex.

A preliminary model for the actin−Tβ_4 complex has been constructed based on the crystallographic structure of the actin monomer (*10*) and incorporating the present data from cross-linking and spectroscopy (Figure 6). The structure of thymosin β_4 was modeled as an extended chain, except for the α-helical region extending from residues 5 to 16, and was then manually rearranged to allow contacts with actin corresponding to the identified cross-links. The α-helical segment of thymosin β_4 has been positioned in the hydrophobic pocket on the barbed end, which is also the major site of contact for profilin (*12*) and gelsolin segment 1 (*11*), and for subdomain 2 of the adjacent actin monomer in F-actin (*42*). The available data put few constraints on the conformation of thymosin β_4 residues 19−43 when bound to actin. The distance between the N-terminus of actin and Gln-41 is about 50 Å, but the length of a 20 residue peptide, if fully extended, is ~70 Å, which would allow it to follow a curved or segmented path along the actin surface between the two points of contact. We cannot exclude the possiblity that part of this region is not in contact with actin. The available data are not sufficient to show whether this region of thymosin β_4 adopts a unique conformation or follows a single path on the actin surface. The model shown in Figure 6 is consistent with the available data, but is necessarily speculative in its details.

The placement of the Tβ_4 helical segment on the barbed end of actin is consistent with the reported cross-linking of thymosin β_9 to actin Cys-374, and with the observed enhancement of the fluorescence of a bimanyl fluor bound to actin Cys-374 in response to β-thymosin binding (*5*). More recently, Reichert et al. (*43*) used a ~9 Å long bifunctional thiol reagent to form disulfide cross-links between thiols on actin and Cys residues in several different mutant thymosin β_4 sequences. The observation that actin Cys-374 could be cross-linked to a thymosin β_4 variant substituted with Cys at residue 6, but not with with Cys at positions 17, 28, 34, or 40, is consistent with the contacts that we have identified. Reichert et al. (*43*) also reported that ATPγS, while bound to actin, could be coupled through the same bifunctional thiol reagent to thymosin β_4 variants substituted with Cys at residues 17 and 28; this result is not consistent with the present results, which place Tβ_4 Lys-18 adjacent to the N-terminus of actin, more than 20 Å away from the nucleotide-binding cleft. Since the affinities of Cys^{17}-Tβ_4 and Cys^{28}-Tβ_4 for actin, as determined by inhibition of polymerization, are respectively about 6-fold and 3-fold lower than that of native thymosin β_4, we suggest that the reaction observed between ATPγS and these thymosin β_4 variants does not reflect the native structure of the actin−Tβ_4 complex and occurred when one or both of the reactants was dissociated from actin.

The structural data indicate that thymosin β_4, like DNase I, profilin, and gelsolin, inhibits actin polymerization by a steric mechanism. Like gelsolin and profilin, thymosin β_4 blocks the barbed end of the actin monomer. In addition, thymosin β_4, like DNase I, contacts the pointed end of the

actin monomer on subdomain 2. The contact identified by cross-linking, actin Gln-41, is at the edge of an actin−actin interface in the filament model of Lorenz et al. (*42*), and can be cross-linked to Lys-113 on subdomain 1 of the adjacent monomer in the same long-pitch helical strand (*44*); these results suggest that the contact between thymosin β_4 and subdomain 2 may sterically block the pointed end of the actin monomer.

Residues 17−25 of thymosin β_4, LKKTETQEK, are homologous in sequence with part of the actobindin sequence, LKHAETVDK, which occurs as part of a tandem repeat at residues 15−23 and 51−59 (*45*). Both Lys-16 and Lys-52 of actobindin can be cross-linked to one of the four N-terminal acidic residues of actin (*46*), in homology with the cross-link between Tβ_4 Lys-18 and actin residues 1−4. In contrast with thymosin β_4, however, Lys-16 of actobindin cross-links more avidly to actin Glu-100, a residue to which thymosin β_4 does not cross-link. The cross-linking study on actobindin gives no indication of whether actobindin blocks the barbed end of actin, but hydrodynamic and spectroscopic studies on the interaction of actobindin with actin (*47*−*49*) indicate that actobindin inhibits actin polymerization by inhibiting nucleation, a mechanism different from the actin-sequestering actvity of thymosin β_4. Thus, actobindin and thymosin β_4, despite sharing sequence homology and predominantly unfolded structures (*46*), may serve different functions related to the control of actin polymerization.

The rate of nucleotide exchange is likely to depend on the conformation of the nucleotide-binding cleft. A computational simulation suggests that the cleft can be opened and closed by movement between the two major domains of actin (*50*). Crystallographic structures obtained under different conditions reveal both "open" (*13*) and "closed" conformations for the cleft (*10*−*12*). Thus, it is likely that actin monomer-binding proteins influence the rate of nucleotide exchange by stabilizing a particular conformation of the nucleotide-binding cleft, and that thymosin β_4, like DNase I and gelsolin but unlike profilin, favors the "closed" conformation.

Conversely, several studies using a variety of methods have shown that the identity of the bound nucleotide influences actin conformation (*40, 51*−*54*). Since the present data apparently exclude any direct contact between thymosin β_4 and the bound nucleotide, it is likely that the greater affinity of thymosin β_4 for ATP−actin versus ADP−actin (*55*) results from nucleotide-induced differences in the conformation of the actin monomer.

The affinity of thymosin β_4 for platelet (predominantly β-isoform) actin is 3−5-fold higher than for skeletal (α-) actin [K_d = 0.4−0.7 μM for platelet vs 2.1 μM for skeletal (*3*)]. The α- and β-actin sequences differ at 25 residues, and inspection of crystallographic structures shows that 15 of the residues which differ in β-actin are accessible on the surface. Of these 15 residues, 10 may potentially make contact with thymosin β_4: in subdomain 1, residues 1 (deleted in β-actin), 2 (Glu to Asp), 4 (Glu to Asp), 5 (Thr to Ile), 6 (Thr to Ala), 16 (Leu to Met), 358 (Thr to Ser), and 365 (Ala to Ser); in subdomain 2, on the "back" face of the monomer, 76 (Ile to Val) (Figure 6). Actin residues 1−6 are already implicated by cross-linking as being close to, if not part of, the contact at the N-terminus of actin, while residues 358 and 365 are within the hydrophobic pocket on the barbed end of actin, which we have proposed as the binding site for the α-helical segment of thymosin β_4. Actin residue 16 or 76 could potentially interact with thymosin β_4 depending on the path Tβ_4 follows between the N-terminus of actin and its contact at Gln-41. Several of these substitutions involve significant changes in hydrophobicity, while the substitutions at residues 1−6 involve significant changes in side-chain orientation (*12*), and both these factors could contribute to the observed difference in affinity.

Comparisons of actin binding by different β-thymosin isoforms, chemically modified β-thymosins, and designed mutants have been reported by several groups (*4, 6*−*8, 38, 56, 57*). The affinity of thymosin β_4 homologues for actin is reduced 20−50-fold by deletion of 6 residues at the N-terminus or 13 residues at the C-terminus (*4, 8, 56*); this result is consistent with the present finding that residues near both termini can be cross-linked to actin. The binding of the N-terminal third of thymosin β_4 to actin depends primarily on hydrophobic contacts, since substitutions at charged residues at positions 1−12 have little effect on actin binding as long as the α-helical structure of this segment is not disrupted; however, reducing the hydrophobicity of this region either by sequence substitution or by oxidation of Met-6 significantly reduces binding (*4, 7, 38, 56, 57*).

Replacement of any of the lysine residues at positions 14, 16, 18, and 19 significantly reduces actin binding; substitution of alanine for Lys-18 increased the K_d for muscle actin to 75 μM (*38, 56*). These results indicate that electrostatic attraction is critical for binding in this region, and are consistent with the high rate of cross-linking observed between Tβ_4 Lys-18 and the actin N-terminus.

Comparison with Other Structures. In protein−protein complexes, the interface typically occupies ~10^3 Å^2 on the surface of each subunit, contains a high proportion of hydrophobic amino acids, and largely excludes solvent; the packing of side chains at an interface is comparable in density to the interior of a protein (*58*). The α-helical segment of thymosin β_4 is the only compactly folded region, and its hydrophobic face may form a miniature solvent-excluding interface with the hydrophobic pocket on the barbed-end surface of subdomains 1 and 3, but the area of this contact would be only ~100−200 Å^2. The limited area of this contact, and the observation that the affinity of thymosin β_4 for actin is sharply reduced by truncation at residue 30 (*56*), indicates that residues throughout the sequence contribute binding energy.

In all well-characterized peptide−receptor complexes, the bound region of the peptide is buried in a cleft on the receptor; in different complexes, 40−100% of the peptide surface area is buried (*59*). Since most of thymosin β_4 remains independently mobile and many side chains undergo little change in environment when bound to actin, it seems unlikely that any substantial fraction of it becomes buried. Instead, binding outside the α-helical region is likely to occur through a string of individual electrostatic and hydrophobic contacts between side chains. The actin−Tβ_4 complex thus does not fit either of the common paradigms for protein−protein or protein−peptide interaction.

ACKNOWLEDGMENT

Mass spectroscopy and protein sequencing were performed at the Protein Chemistry Facility of the Department of Pathology and Laboratory Medicine, University of Pennsylvania. Amino acid analysis and protein sequencing were

performed at the Protein Microchemistry Core Facility of the Wistar Institute. Molecular modeling was performed at the University of Pennsylvania Cancer Center Computer Facility. D.S. thanks Rajasree Golla for assistance in the lab, Georgi Kostov, Kelly Gallagher, and Kim Sharp for help with computational modeling, and Vivianne Nachmias, Walter Englander, and William T. Moore for many helpful discussions and much-needed encouragement.

REFERENCES

1. Safer, D., Nachmias, V. T., and Golla, R. (1990) *Proc. Natl. Acad. Sci. U.S.A. 87*, 2536−2540.
2. Safer, D., Elzinga, M., and Nachmias, V. T. (1991) *J. Biol. Chem. 266*, 4029−4032.
3. Weber, A., Nachmias, V. T., Pennise, C. R., Pring, M., and Safer, D. (1992) *Biochemistry 31*, 6179−6185.
4. Hannappel, E., and Wartenberg, F. (1993) *Biol. Chem. Hoppe-Seyler 374*, 117−122.
5. Heintz, D., Reichert, A., Mihelic, M., Voelter, W., and Faulstich, H. (1993) *FEBS Lett. 329*, 9−12.
6. Yu, F.-X., Lin, S.-C., Morrison-Bogorad, M., Atkinson, M. A. L., and Yin, H. L. (1993) *J. Biol. Chem. 268*, 502−509.
7. Jean, C., Rieger, K., Blanchoin, L., Carlier, M.-F., Lenfant, M., and Pantaloni, D. (1994) *J. Muscle Res. Cell Motil. 15*, 278−286.
8. Huff, T., Zerzawy, D., and Hannappel, E. (1995) *Eur. J. Biochem. 230*, 650−657.
9. Safer, D., and Chowrashi, P. K. (1995) *Mol. Biol. Cell 6*, 23a.
10. Kabsch, W., Mannherz, H.-G., Suck, D., Pai, E. F., and Holmes, K. C. (1990) *Nature 347*, 37−44.
11. McLaughlin, P. J., Gooch, J. T., Mannherz, H.-G., and Weeds, A. G. (1993) *Nature 364*, 685−692.
12. Schutt, C. E., Myslik, J. C., Rozycki, M. D., Goonesekere, N. C. W., and Lindberg, U. (1993) *Nature 365*, 810−816.
13. Chik, J. K., Lindberg, U., and Schutt, C. E. (1996) *J. Mol. Biol. 263*, 607−623.
14. Hatanaka, H., Ogura, K., Moriyama, K., Ichikawa, S., Yahara, I., and Inagaki, F. (1996) *Cell 85*, 1047−1055.
15. Hitchcock, S. E. (1980) *J. Biol. Chem. 255*, 5668−5673.
16. Mannherz, H. G., Goody, R. S., Konrad, M., and Nowak, E. (1980) *Eur. J. Biochem. 104*, 367−379.
17. Harris, H. E. (1985) *FEBS Lett. 190*, 81−83.
18. Tellam, R. L. (1986) *Biochemistry 25*, 5799−5804.
19. Hawkins, M., Pope, B., Maciver, S. K., and Weeds, A. G. (1993) *Biochemistry 32*, 9985−9993.
20. Hayden, S. M., Miller, P. S., Brauweiler, A., and Bamburg, J. R. (1993) *Biochemistry 32*, 9994−10004.
21. Goldschmidt-Clermont, P.-J., Furman, M. I., Wachsstock, D., Safer, D., Nachmias, V. T., and Pollard, T. D. (1992) *Mol. Biol. Cell 3*, 1015−1024.
22. Mockrin, S. C., and Korn, E. D. (1980) *Biochemistry 19*, 5359−5362.
23. Czisch, M., Schleicher, M., Horger, S., Voelter, W., and Holak, T. A. (1993) *Eur. J. Biochem. 218*, 335−344.
24. Safer, D., and Elzinga, M. (1996) *Biophys. J. 70*, A125.
25. Pardee, J. D., and Spudich, J. A. (1982) *Methods Enzymol. 85*, 164−181.
26. Nachmias, V. T., Cassimeris, L., Golla, R., and Safer, D. (1993) *Eur. J. Cell Biol. 61*, 314−320.
27. Smith, P. K., Krohn, R. I., Hermanson, G. T., Mallia, A. K., Gartner, F. H., Provenzano, M. D., Fujimoto, E. K., Goeke, N. M., Olson, B. J., and Klenk, D. C. (1985) *Anal. Biochem. 150*, 76−85.
28. Piotto, M., Saudek, V., and Sklenar, V. (1992) *J. Biomol. NMR 2*, 661−665.
29. Takashi, R. (1988) *Biochemistry 27*, 938−943.
30. Dixon, H. B. F., and Perham, R. N. (1968) *Biochem. J. 109*, 312−314.
31. Chen, Y.-H., Yang, J. T., and Chau, K. H. (1974) *Biochemistry 13*, 3350−3359.
32. Johnson, W. C. (1990) *Proteins: Struct., Funct., Genet. 7*, 205−214.
33. Wuthrich, K. (1986) *NMR of Proteins and Nucleic Acids*, John Wiley & Sons, New York.
34. Barden, J. A., Cooke, R., Wright, P. E., and dos Remedios, C. G. (1980) *Biochemistry 19*, 5912−5916.
35. Highsmith, S., and Jardetzky, O. (1980) *FEBS Lett. 121*, 55−60.
36. Folk, J. E., and Chung, S. I. (1985) *Methods Enzymol. 113*, 358−375.
37. Zarbock, J., Oschkinat, H., Hannappel, E., Kalbacher, H., Voelter, W., and Holak, T. A. (1990) *Biochemistry 29*, 7814−7821.
38. Van Troys, M., Dewitte, D., Goethals, M., Carlier, M.-F., Vandekerckhove, J., and Ampe, C. (1996) *EMBO J. 15*, 201−210.
39. Feinberg, J., Heitz, F., Benyamin, Y., and Roustan, C. (1996) *Biochem. Biophys. Res. Commun. 222*, 127−132.
40. Moraczewska, A., Strzelecka-Golaszewska, H., Moens, P. D. J., and dos Remedios, C. G. (1996) *Biochem. J. 317*, 605−611.
41. Kim, E., Miller, C. J., Motoki, M., Seguro, K., Muhlrad, A., and Reisler, E. (1996) *Biophys. J. 70*, 1439−1446.
42. Lorenz, M., Popp, D., and Holmes, K. C. (1993) *J. Mol. Biol. 234*, 826−836.
43. Reichert, A., Heintz, D., Echner, H., Voelter, W., and Faulstich, H. (1996) *J. Biol. Chem. 271*, 1301−1308.
44. Hegyi, G., Michel, H., Shabanowitz, J., Hunt, D. F., Chatterjie, N., Healy-Louie, G., and Elzinga, M. (1992) *Protein Sci. 1*, 132−144.
45. Vandekerckhove, J., Van Damme, J., Vancompernolle, K., Bubb, M. R., Lambooy, P. K., and Korn, E. D. (1990) *J. Biol. Chem. 265*, 12801−12805.
46. Vancompernolle, K., Vandekerckhove, J., Bubb, M. R., and Korn, E. D. (1991) *J. Biol. Chem. 266*, 15427−15431.
47. Bubb, M. R., Lewis, M. S., and Korn, E. D. (1991) *J. Biol. Chem. 266*, 3820−3826.
48. Bubb, M. R., Lewis, M. S., and Korn, E. D. (1994a) *J. Biol. Chem. 269*, 25587−25591.
49. Bubb, M. R., Knutson, J. R., Porter, D. K., and Korn, E. D. (1994b) *J. Biol. Chem. 269*, 25592−25597.
50. Tirion, M. M., and ben-Avraham, D. (1993) *J. Mol. Biol. 230*, 186−195.
51. Janmey, P. A., Hvidt, S., Oster, G. F., Lamb, J., Stossel, T. P., and Hartwig, J. H. (1990) *Nature 347*, 95−99.
52. Orlova, A., and Egelman, E. H. (1992) *J. Mol. Biol. 227*, 1043−1053.
53. Lepault, J., Ranck, J.-L., Erk, I., and Carlier, M.-F. (1994) *J. Struct. Biol. 112*, 79−91.
54. Kim, E., Motoki, M., Seguro, K., Muhlrad, A., and Reisler, E. (1995) *Biophys. J. 69*, 2024−2032.
55. Carlier, M.-F., Jean, C., Rieger, K. J., Lenfant, M., and Pantaloni, D. (1993) *Proc. Natl. Acad. Sci. U.S.A. 90*, 5034−5038.
56. Vancompernolle, K., Goethals, M., Huet, C., Louvard, D., and Vandekerckhove, J. (1992) *EMBO J. 11*, 4739−4746.
57. Heintz, D., Reichert, A., Mihelic-Rapp, M., Stoever, S., Voelter, W., and Faulstich, H. (1994) *Eur. J. Biochem. 223*, 345−350.
58. Janin, J., and Chothia, C. (1990) *J. Biol. Chem. 265*, 16027−16030.
59. Stanfield, R. L., and Wilson, I. A. (1995) *Curr. Opin. Struct. Biol. 5*, 103−113.

BI970185V